Discussion on Spikes and Plateaus in Pulse Distortion Shape Along Exponential Microstrip Taper

Yue Peng Yan and Masanori Kobayashi

***Abstract*—The propagation distortions of a nonideal square pulse along an exponential microstrip taper have been numerically calculated. Each part of the distorted pulse shape is related to either the frequency-dependent characteristics of the effective relative permittivity or to the frequency-dependent reflection coefficient characteristics. The components of signal spectra at frequencies below 9 Grad/s do not cause the ringing distortions, but cause the upward slope shift in the center part and the upward parallel shift in the sustained tail part to the distorted pulse shape for the case of no reflection (NR). The ringing distortions and the large spikes of the overshoot and undershoot distortions are caused by the components of the signal spectra in the frequency range $100 \leq \omega \leq 200$ Grad/s where the effective relative permittivity is changing very quickly with frequency.**

***Index Terms*—Distortion, microstrip taper, multiple reflections, pulse.**

I. Introduction

In microwave integrated circuits (MIC's), monolithic microwave integrated circuits (MMIC's), and high-speed digital circuits, ultrashort electric signals or high switching speeds are now available. Those spectra extend into the dispersive frequency regions of microstrip transmission lines. Therefore, analyzing distortion is important because the distortion significantly alters the form of a pulse as it propagates down the line. It has also been investigated by a number of researchers [1]–[5].

A tapered microstrip transmission line has been used in MIC's for impedance transformation. The characteristic impedance is distance dependent in the tapered line. This distance-dependent characteristic impedance causes multiple reflections in the tapered line. Therefore, the pulse distortions are caused by both the retarded time owing to the frequency-dependent phase velocity and the multiple reflection owing to the distance-dependent characteristic impedance [5]–[9]. Reference [6] described the following results: the large and sharp peaks in the distorted wave are caused by the frequency-dispersive permittivity, and the sustained tail and slope of the plateau in the distorted wave are caused by multiple reflections in the tapered line.

However, the detailed theoretical discussion for these results was not given in [6].

II. Plateau Distortions

Consider the exponential tapered microstrip transmission line shown in Fig. 1, which is identical to the transmission line analyzed in [6] and [10]. Numerically calculating the pulse distortions along the tapered line requires the values of the phase velocity and the characteristic impedance at position z. Let those values be approximated by those of a uniform line having the same sectional dimension as the taper has at that point. To simplify the analysis, this paper assumes that the characteristic impedance is independent of frequency. The phase velocity and the characteristic impedance can be obtained using the method shown in [6] and [10].

Manuscript received March 4, 1997; revised April 7, 1998.

The authors are with the Department of Electrical and Electronic Engineering, Faculty of Engineering, Ibaraki University, Hitachi, Ibaraki 316, Japan.

Publisher Item Identifier S 0018-9480(98)04945-X.

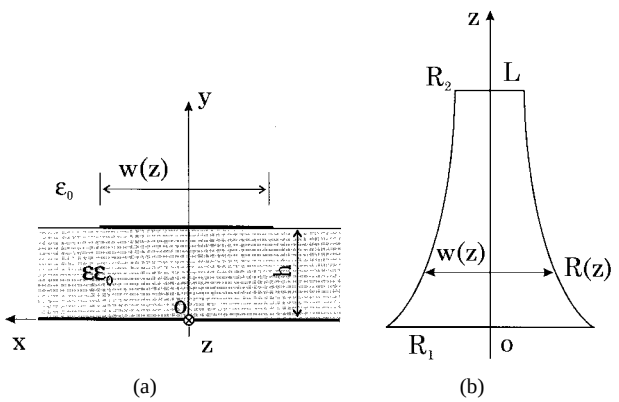

Fig. 1. Exponential microstrip taper. (a) Cross section. (b) Configuration of strip conductor.

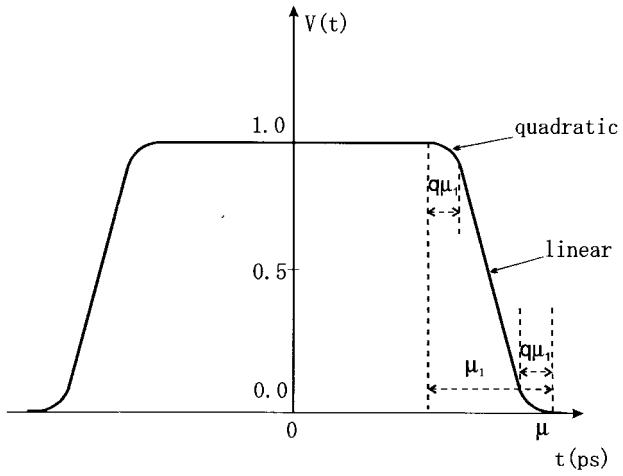

Fig. 2. Nonideal square pulse.

The distorted signal $v(t, z = L)$ received at $z = L$ can be obtained as follows [6]:

$$v(t, z = L) = \frac{1}{2\pi} \int_{-\infty}^{\infty} V(\omega, z = 0_-) \cdot [1 + \rho(\omega)] e^{j\omega[t - \tau_L(\omega)/2]}\, d\omega \quad (1)$$

where $V(\omega, z = 0_-)$ denotes the Fourier transform of the sending signal $v(t, z = 0_-)$, $\rho(\omega)$ the input reflection coefficient, and $\tau_L(\omega)/2$ the propagation time.

This paper discusses the frequency-dependent pulse distortions for the case of a nonideal square pulse [5], shown in Fig. 2, along the exponential microstrip taper, shown in Fig. 1. The parameters of the nonideal square pulse are taken by $2\mu = 200$ ps, $\mu_1 = 20$ ps, and $q = 0.12$. The parameters of the exponential taper are taken by $\epsilon = 8$, $h = 1$ mm, $L = 50$ mm, $R_1 = 63.58\ \Omega$ ($w/h = 0.7$ at $z = 0$), and $R_2 = 117.99\ \Omega$ ($w/h = 0.1$ at $z = L$). These parameters are identical to those of the case described in [6] and [10]. This small range of w/h and the value of $\epsilon = 8$ are taken for simplicity in the calculation because the results obtained in [6] and [10] are used in this paper. Fig. 3 shows the input reflection coefficient $|\rho(\omega)|$ and the propagation time $\tau_L(\omega)/2$ versus angular frequency ω.

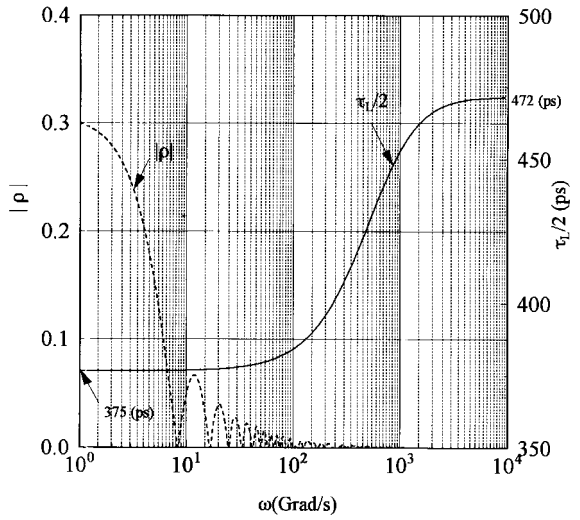

Fig. 3. Input reflection coefficient $|\rho(\omega)|$ and propagation time $\tau_L(\omega)/2$.

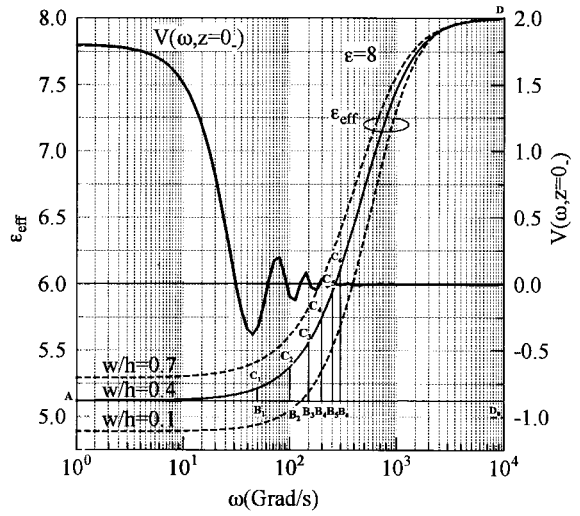

Fig. 4. Spectra of nonideal square pulse $V(\omega, z = 0_-)$ and dispersive characteristics of effective relative permittivity ϵ_{eff} for microstrip lines with $w/h = 0.1, 0.4, 0.7 (\epsilon = 8)$. Effective relative permittivity is the function of both the angular frequency ω and the position z for the exponential taper. That curved surface of $\epsilon_{\text{eff}}(\omega, z)$ for two variables ω and z can be easily visualized using the three curves for microstrip lines. $\epsilon_{\text{eff}}(\omega, z)$ is used in obtaining the results shown in Fig. 5: v_j; $A \rightarrow B_j \rightarrow C_j \rightarrow D$, $j = 1, 2, 3, 4, 5, 6$, v_0; $A \rightarrow D_0$, v_f; $A \rightarrow C_1 \rightarrow C_2 \rightarrow \cdots \rightarrow C_6 \rightarrow D$ at the position z having $w/h = 0.4$ as the example in the exponential taper.

The spectrum of a nonideal square pulse $V(\omega, z = 0_-)$ is shown in Fig. 4. Reference [6] showed that the plateau distortions in the center and sustained tail parts of distorted pulse shape are caused by multiple reflections in the tapered line. To pursue in detail the frequency dependence of the plateau distortions, this paper replaces $\rho(\omega)$ in (1) by the reflection coefficient $\rho_j(\omega)$ obtained by letting $\rho(\omega) = 0$ as follows:

$$\rho_j(\omega) = \begin{cases} 0, & |\omega| \le \omega_j \\ \rho(\omega), & |\omega| > \omega_j. \end{cases} \tag{2}$$

The pulse distortions $v_1(t, z = L)$, $v_2(t, z = L)$, and $v_3(t, z = L)$ were numerically calculated for three cases of $\omega_1 = 1$ Grad/s, $\omega_2 = 4$ Grad/s, and $\omega_3 = 9$ Grad/s, respectively. Fig. 5 shows those results. The dashed lines are the pulse distortions $v_1(t, z = L)$, $v_2(t, z = L)$, and $v_3(t, z = L)$. The dotted line is the pulse distortion $v_0(t, z = L)$ for the case of no reflection (NR) where $\rho(\omega) \equiv 0$ for all frequency. The solid line is the pulse distortion $v(t, z = L)$ where $\rho(\omega) \neq 0$ for all ω. The difference between curves v and v_j represents the contribution of the components $0 \le |\omega| \le \omega_j$ on the distortion shape. The difference between curves v_j and v_0 represents the contribution of the components $|\omega| > \omega_j$ on the distortion shape. Moreover, the difference between curves v_j and v_k represents the contribution of the components $\omega_j \le |\omega| \le \omega_k$ on the distortion shape.

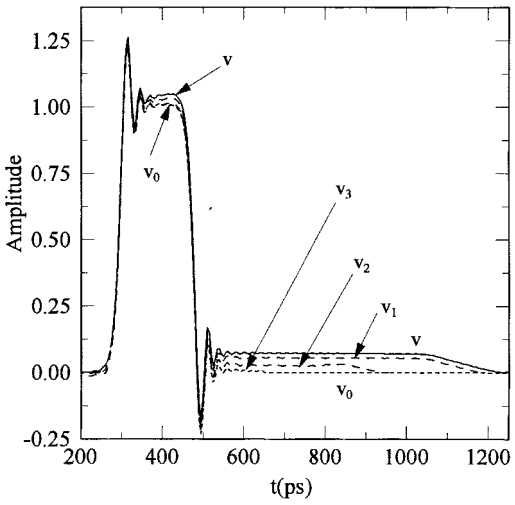

Fig. 5. Influence of reflection coefficients on distorted pulse shapes. $v_1(t, z = L)$ when $\rho(\omega) = 0$ for $\omega \le 1$ Grad/s. $v_2(t, z = L)$ when $\rho(\omega) = 0$ for $\omega \le 4$ Grad/s. $v_3(t, z = L)$ when $\rho(\omega) = 0$ for $\omega \le 9$ Grad/s. $v_0(t, z = L)$ when $\rho(\omega) \equiv 0$. $v(t, z = L)$ when $\rho(\omega) \neq 0$.

In Fig. 5, curves v_0 and v_3 cannot be distinguished from each other. This shows that the plateau distortions in the center and tail parts of the distortion shape are caused by the multiple reflections in the low-frequency range below 9 Grad/s. The lower the frequency, the larger the reflection coefficient, as shown in Fig. 3, and the larger the plateau distortions, as shown in Fig. 5.

Note, however, that the curves v, v_1, v_2, and v_3 have the same ringing shapes as curve v_0. This implies that the components of spectra below 9 Grad/s do not cause the ringing distortions. This is because the propagation time $\tau_L(\omega)/2$ does not change in the low-frequency range below 9 Grad/s, as shown in Fig. 3.

III. Spike Distortions

To pursue in detail the frequency dependence of the spikes of the overshoot and undershoot distortions, this paper considers the effective relative permittivity $\epsilon_j(\omega, z)$ obtained by letting

$$\epsilon_j(\omega, z) = \begin{cases} \epsilon_{\text{eff}}(\omega = 0, z), & |\omega| \le \omega_j \\ \epsilon_{\text{eff}}(\omega, z), & |\omega| > \omega_j. \end{cases} \tag{3}$$

Therefore, the propagation time $\tau_L(\omega)/2$ in (1) is replaced by $\tau_j(\omega)/2$, which is obtained as follows:

$$\tau_j(\omega)/2 = \int_0^L \frac{c}{\sqrt{\epsilon_j(\omega, z)}}\, dz. \tag{4}$$

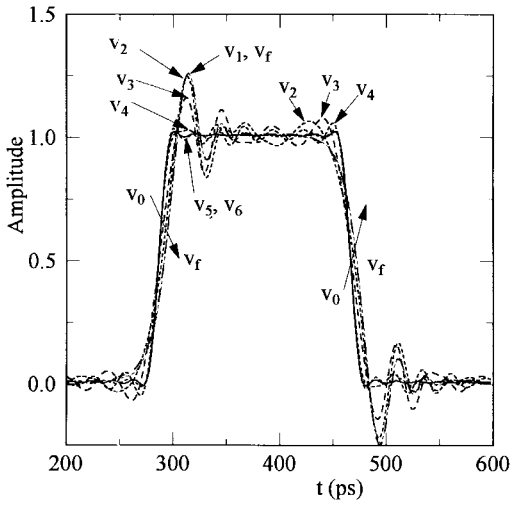

Fig. 6. Influence of each part in dispersive characteristics of effective relative permittivity on the large and sharp spikes in the distortion shape (NR). v_j: $\epsilon_{\rm eff}(0,\ z)$ in $0 \le \omega \le \omega_j$, $j = 1, 2, 3, 4, 5, 6$, $\omega_1 = 50$, $\omega_2 = 100$, $\omega_3 = 150$, $\omega_4 = 200$, $\omega_5 = 250$, $\omega_6 = 300$ Grad/s. v_0: $\epsilon_{\rm eff}(0,\ z)$ (no dispersion). v_f: $\epsilon_{\rm eff}(\omega,\ z)$ (full dispersion).

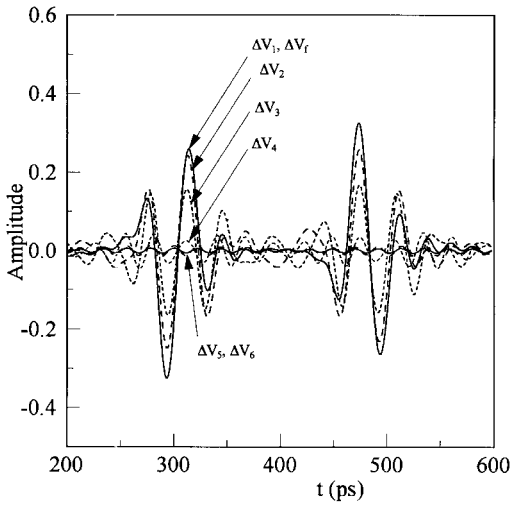

Fig. 7. Curve for the differences $\Delta v_j = (v_j - v_0)$, $j = 1, 2, 3, 4, 5, 6$.

The numerical calculations for (1) using (4) were carried out by taking temporarily $\rho(\omega) \equiv 0$ (NR) in (1) to remove the distortion caused by the multiple reflection because the influence of the multiple reflection on the distorted pulse shape was clarified in Section II.

The pulse distortions $v_1(t,\ z = L)$, $v_2(t,\ z = L), \cdots$, and $v_6(t,\ z = L)$, shown in Fig. 6, are the results numerically calculated for six cases of $\omega_1 = 50$ Grad/s, $\omega_2 = 100$ Grad/s, $\omega_3 = 150$ Grad/s, $\omega_4 = 200$ Grad/s, $\omega_5 = 250$ Grad/s, and $\omega_6 = 300$ Grad/s, respectively. The curve $v_0(t,\ z = L)$, shown in Fig. 6, is the result for the case of no dispersion. The curve $v_f(t,\ z = L)$ is the result for the case of full dispersion. The curve v_1 cannot be distinguished from the curve v_f (full dispersion), but the curve v_2 can be distinguished from the curve v_f. Therefore, the spikes of the overshoot and undershoot distortions begin to be caused from the frequency components of ω about 100 Grad/s. Curve v_3 is illustrated between curves v_2 and v_4. Curve v_4 approaches curve v_0 (no dispersion). Curves v_5 and v_6 closely follow curve v_0. Therefore, the greatest influence on the large and sharp spikes in the distortion shape is caused by the components of spectra in the frequency range $100 \le \omega \le 200$ Grad/s, where the effective relative permittivity $\epsilon_{\rm eff}$ is changing very quickly with frequency, as shown in Fig. 4, for the case of microstrip lines. The effective relative permittivity $\epsilon_{\rm eff}(\omega,\ z)$ of the exponential tapered line is the function of both the angular frequency ω and the position z. That curved surface of $\epsilon_{\rm eff}(\omega,\ z)$ for two variables ω and z can be easily visualized using the three curves for microstrip lines, as shown in Fig. 4.

The differences $\Delta v_j = (v_j - v_0)$ are illustrated in Fig. 7 and clarify that the spikes are caused by the frequency components $100 \le \omega \le 200$ Grad/s. Curves Δv_5 and Δv_6 show only very small ringing. This means that the components of frequency $\omega \ge 250$ Grad/s exert only very slight influence on the distortion shape. Even though this high-frequency range $\omega \ge 250$ Grad/s has large dispersion of effective relative permittivity, the spectra of the signal is very small in this region, as shown in Fig. 4.

IV. Conclusions

The spikes and plateaus in the propagation distortions have been discussed for the nonideal square pulse along the exponential taper. It has been clarified that $\rho(\omega)$ controls the plateau slope and slow tail response, and $\epsilon(\omega)$ controls the large spikes and ringing distortions.

Acknowledgment

The authors would like to thank the reviewers for their valuable advice and helpful corrections to this paper's grammar.

References

[1] R. L. Veghte and C. A. Balanis, "Dispersion of transient signals in microstrip transmission lines," *IEEE Trans. Microwave Theory Tech.*, vol. MTT-34, pp. 1427–1436, Dec. 1986.

[2] T. Leung and C. A. Balanis, "Attenuation distortion of transient signals in microstrip," *IEEE Trans. Microwave Theory Tech.*, vol. 36, pp. 765–769, Apr. 1988.

[3] ——, "Pulse dispersion distortion in open and shielded microstrip using the spectral-domain method," *IEEE Trans. Microwave Theory Tech.*, vol. 36, pp. 1223–1226, July 1988.

[4] J. P. Gilb and C. A. Balanis, "Pulse distortion on multilayer coupled microstrip lines," *IEEE Trans. Microwave Theory Tech.*, vol. 37, pp. 1620–1628, Oct. 1989.

[5] P. Pramanick and R. P. Mansour, "Dispersion characteristics of square pulse with finite rise time in single, tapered, and coupled microstrip lines," *IEEE Trans. Microwave Theory Tech.*, vol. 39, pp. 2117–2122, Dec. 1991.

[6] M. Kobayashi and Y. Nemoto, "Analysis of pulse dispersion distortion along exponential and Tchebycheff microstrip tapers," *IEEE Trans. Microwave Theory Tech.*, vol. 42, pp. 834–839, May 1994.

[7] Y. P. Tang, Z. Li, and S. Y. Tang, "Transient analysis of tapered transmission lines used as transformers for short pulses," *IEEE Trans. Microwave Theory Tech.*, vol. 43, pp. 2573–2578, Nov. 1995.

[8] E. J. Park, "An efficient synthesis technique of tapered transmission line with loss and dispersion," *IEEE Trans. Microwave Theory Tech.*, vol. 44, pp. 462–465, Mar. 1996.

[9] Y. P. Tang and S. Y. Tang, "Transient analysis of tapered lines based on the method of series expansion," *IEEE Trans. Microwave Theory Tech.*, vol. 44, pp. 1742–1744, Oct. 1996.

[10] M. Kobayashi and N. Sawada, "Analysis and synthesis of tapered microstrip transmission lines," *IEEE Trans. Microwave Theory Tech.*, vol. 40, pp. 1642–1646, Aug. 1992.